One-dimensional mathematical and numerical modeling of liquid dynamics in a horizontal capillary

Giovanni Cavaccini[a], Vittoria Pianese[a], Alessandra Jannelli[b], Salvatore Iacono[b] and
Riccardo Fazio[b,*]
[a]*Alenia Aeronautica, viale dell'Aeronautica s.n.c. 80038 Pomigliano d'Arco – Napoli, Italy*
[b]*Department of Mathematics, University of Messina, Salita Sperone 31, 98166 Messina, Italy*

Abstract. This paper is concerned with a mathematical and numerical study of liquid dynamics in a horizontal capillary. We derive a two-liquids model for the prediction of capillary dynamics. This model takes into account the effects of real phenomena: like the outside flow action, or the entrapped gas inside a closed-end capillary. Moreover, the limitations of the one-dimensional model are clearly indicated. Finally, we report on several tests of interest: an academic test case that can be used to check available numerical methods, a test for decreasing values of the capillary radius, a simulation concerning a closed-end capillary, and two test cases for two liquids flow.

In order to study the introduced mathematical model, our main tool, is a reliable one-step adaptive numerical approach based on a one-step one-method strategy.

1. Introduction

At the beginning of the nineteenth century Young and Laplace, working independently, were the first to report on theoretical studies concerning surface tension and capillarity. Their work, made approximatively at the same time, reported that the static pressure on the liquid side of a liquid-air interface is reduced by the effect of the surface tension. Later, Hagen and Poiseuille studying the flow of viscous liquids in circular pipes (and capillary tubes in particular), derived the well-known Poiseuille flow profile for a, fully developed, Newtonian fluid. Reynolds tested experimentally the stability of the Poiseuille profile, and he found that it held in the case of laminar flow.

Starting from the beginning of the last century several publications were devoted to study the dynamics of liquid flow into a capillary, leading to the derivation of the celebrated Washburn solution, the Bosanquet model, and, more recently, to the Szekely-Neumann-Chang (SNC) model. Bell and Cameron [2], Lucas [21], Washburn [31], and Rideal [25] considered the liquid penetration as being determined by

---

*Corresponding author. E-mail: rfazio@dipmat.unime.it.

a balance among capillarity, gravitational and viscous forces and used the Poiseuille profile as velocity profile. The Washburn solution has been confirmed by a lot of experimental data and also by molecular dynamic simulations, see for instance Martic et al. [22]; it is still considered as a valid approximation, although it fails to describe the initial transient, since it neglects the inertial effects which are relevant at the beginning of the process. The inertial effects were considered in a model proposed by Bosanquet [5]. The SNC model, introduced by Szekely et al. [29], takes into account the outside flow effects including an apparent mass parameter within the inertial terms.

Recently, many experimental and theoretical studies on liquid dynamics due to capillary action have pointed out the short-time limitations of the Washburn solution, but its validity as an asymptotic approximation. For example, liquids flowing in thin tubes have been studied by Fisher and Lark [16], in surface grooves by Mann et al. [18], Romero and Yost [26], Rye et al. [27], and Yost et al. [32], and on micro-strips by Rye et al. [28]. On the other hand, several studies have been devoted to capillary rise, dynamics of menisci, wetting and spreading as well as accommodating the no-slip condition of contact line motions, see for instance the papers by Clanet and Quéré [10], Zhmud et al. [33], the recent book by de Gennet et al. [12] and the references quoted therein. Moreover, useful reviews appeared within the specialized literature by Dussan [14], de Gennes [11], and Leger and Joanny [20].

Our main concern is the mathematical and numerical modeling of horizontal capillaries for two immiscible liquids penetration, see for instance Chan and Yang [9] or Blake and De Coninck [4]. Moreover, we discuss the effect of the entrapped gas on the liquid dynamics, which was studied first by Deutsch [13], from a theoretical viewpoint and, more recently, by Pesse et al. [23] from an experimental one.

Our main tool for studying the introduced mathematical model is an adaptive numerical approach developed by Jannelli and Fazio [17]. The adaptive approach is based on a one-step one-method strategy and, in this paper, for the basic method we use the classical fourth order Runge-Kutta method.

This study is of interest for the non-destructive control named "liquid penetrant testing" used in the production of airplane parts, for instance, as well as in many industrial applications where the detection of open defects is a relevant concern. Liquid penetrants are frequently employed to locate (open) defects in solid or porous materials. The basic technique involves: cleaning the peace to be tested, applying (by immersion) the penetrant, removal of excess penetrant, application of a developer (like an absorbent coating), and visual or computer assisted inspection for detection.

Preliminary reports on the main topic were presented, by the corresponding author, at the International Conference of Computational Methods in Sciences and Engineering (ICCMSE) 2006, see Cavaccini et al. [8], and at the 6th International Congress on Industrial and Applied Mathematics 2007 (ICIAM 07), see Fazio et al. [15].

2. Mathematical modeling

Let us start with the derivation of the governing equation from first principles. With reference to Fig. 1, we consider a column of liquid 1, usually water, of fixed length ℓ_0 entrapped inside a horizontal straight capillary of radius R and finite length L. At the left end of the capillary we have a reservoir filled with a penetrant liquid 2. We are interested in modeling the dynamics of both fluids under the action of the surface tension.

For the validity of a one-dimensional analysis we have to require that the fluid has a quasi-steady Poiseuille velocity profile, that is, the Reynolds number is small: $R_e = RU/\mu \ll 1$. Here U is the average axial velocity inside the capillary, and μ is the liquid viscosity. The Reynolds number relates the
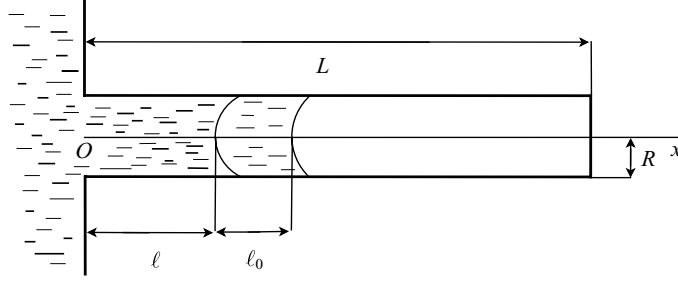
Fig. 1. Draft of a cylindrical capillary section.

inertial forces to viscous ones. Viscosity is related to the internal friction of the fluid and it produces a resistance to shear and a tendency of the fluid to move in parallel layers known as laminar flow. Inertia is a measure of the tendency of a moving body to retain its initial motion, opposing to laminar flow and even resulting in turbulent flow. Moreover, both menisci can be approximated by spherical caps. This condition implies that Bond, Capillary, and Weber numbers are small, that is $Bo = 4\rho g R^2/\gamma \ll 1$, $Ca = \mu_0 U/\gamma \ll 1$, and $We = 2\rho R U^2/\gamma \ll 1$, where ρ and γ are the liquid density and surface tension, respectively, and g is the acceleration due to gravity. The Bond number, which is defined as the ratio of gravitational to surface tension forces, can be used to monitor if gravity is introducing two-dimensional effects into the problem, see Polzin and Choueiri [24] for a full discussion on this topic. The ratio between viscous and capillary forces is given by the capillary number. Capillarity is the rise or depression of a liquid in a small passage, such us a thin tube. Water inside a glass capillary tube will have a concave meniscus that is in equilibrium because of a pressure difference across the interface. Such a pressure difference exists whenever a liquid surface is curved (as in the case of liquid drops or soap bubbles), with the higher pressure found on the inner side of the curve. The Weber number can be thought of as a measure of the relative importance of the fluid's inertia compared to its surface tension. Finally, we use a dynamic contact angle simplification. Such a simplification is valid in the limit of low capillary numbers or when $R/L \ll 1$. A detailed discussion of the dynamic contact angle simplification is provided by Tokaty [30] or Adamson [1].

Assuming that the above requirements are fulfilled, the Newtonian equation of motion can be written as follows

$$\frac{d(mU)}{dt} = F_{\text{drive}} - F_{\text{drag}} \tag{1}$$

where $m(t)$ is the mass of the two liquids, t is the time, and F_{drive} and F_{drag} are drive and drag forces, respectively. We can express the average axial velocity as $U = d\ell/dt$, where ℓ is the moving liquid-liquid interface coordinate, so that the momentum can be specified as

$$\begin{aligned}\frac{d(mU)}{dt} &= m\frac{dU}{dt} + \frac{dm}{dt}U \\ &= \pi R^2 \left(\rho_1 \ell_0 + \rho_2 \ell\right)\frac{d^2\ell}{dt^2} + \pi R^2 \rho_2 \left(\frac{d\ell}{dt}\right)^2\end{aligned} \tag{2}$$

where ρ_1 and ρ_2 are the densities of the two liquids. Moreover, from the Navier-Stokes model written in suitable cylindrical coordinates and applying no slip boundary conditions at the capillary wall, it is

possible to derive the Poiseuille parabolic velocity profile

$$u(r) = \frac{1}{4\mu}\frac{\Delta p}{\Delta z}\left(R^2 - r^2\right) \ , \tag{3}$$

where r is the radial cylindrical coordinate. For a simple derivation of Eq. (3) see Birkhoff [3, p. 36]. The volumetric flow rate is given by

$$Q = \frac{\pi R^4}{8\mu}\frac{\Delta p}{\Delta z}.$$

For a constant area tube Q may also be written

$$Q = \pi R^2 \frac{d\ell}{dt} \ ,$$

so that Eq. (3) can be rewritten as

$$u(r) = 2U\left(1 - \frac{r^2}{R^2}\right). \tag{4}$$

Then, the expression of the viscous drag force is given by

$$\begin{aligned} F_{\mathrm{drag}} &= -2\pi R\left(\mu_1\ell_0 + \mu_2\ell\right)\left.\frac{du}{dr}\right|_{r=R} \\ &= 8\pi\left(\mu_1\ell_0 + \mu_2\ell\right)\frac{d\ell}{dt} \end{aligned} \tag{5}$$

where μ_1 and μ_2 are the dynamic viscosities of the two liquids. The driving force, here due to the surface tension only, can be defined as

$$F_{\mathrm{drive}} = 2\pi R\left(\gamma_1\cos\vartheta_1 + \gamma_{12}\cos\vartheta_{12}\right) \tag{6}$$

where γ_1 and γ_{12} are the surface free energy for the liquid 1-air and the liquid 1-liquid 2 interfaces, and ϑ_1 and ϑ_{12} are corresponding menisci contact angles, see for instance Cartz [7]. At the end of this derivation we get the following second order differential equation

$$\frac{d}{dt}\left[\left(\rho_1\ell_0 + \rho_2(\ell + cR)\right)\frac{d\ell}{dt}\right] = 2\frac{\gamma_1\cos\vartheta_1 + \gamma_{12}\cos\vartheta_{12}}{R} - 8\frac{\mu_1\ell_0 + \mu_2\ell}{R^2}\frac{d\ell}{dt}. \tag{7}$$

Here we have taken into account the coefficient of apparent mass $c = O(1)$, as introduced by Szekely et al. [29]. Moreover, in the case of a vertical capillary, the gravity action should be taken into account, by adding to the right hand side of Eq. (7) the term

$$\pm(\rho_1\ell_0 + \rho_2\ell)g \ , \tag{8}$$

where the plus or minus sign have to be used when the liquid reservoir is over or below the cavity, respectively. Moreover, for a closed-end capillary the entrapped gas action should be taken into account, by adding to the right hand side of Eq. (7) a term

$$\Omega(\ell, L) \ ,$$

depending on the lengths involved.

Equation (7), with suitable initial conditions discussed at length by Kornev and Neimark [19], accounts for the displacement of the two liquids due to the combined surface tensions action of both liquids inside a horizontal capillary. As far as the authors knowledge is concerned, no analytical solutions are available for Eq. (7).

3. A single fluid

In this section we report results, that are already available in literature, for a single fluid case. In the case of a single fluid dynamics, that is $\ell_0 = 0$, the Eq. (7), omitting also all subscripts related to the considered fluid properties, becomes

$$\rho(\ell + cR)\frac{d^2\ell}{dt^2} + \rho\left(\frac{d\ell}{dt}\right)^2 = 2\frac{\gamma\cos\vartheta}{R} - 8\frac{\mu\ell}{R^2}\frac{d\ell}{dt} + \Omega(\ell, L). \tag{9}$$

If $\Omega = 0$, then one exact solution for Eq. (9) is given by

$$\ell^2 = \frac{R\gamma\cos\vartheta}{\mu}t - \frac{R^3\gamma\rho}{8\mu^2}\exp\left(-\frac{8\mu}{R^2\rho}t\right). \tag{10}$$

3.1. Washburn solution

Within a steady flow assumption, that is omitting the left hand side inertial terms, and considering an open end capillary, $\Omega = 0$, Eq. (9) reduces to

$$\ell\frac{d\ell}{dt} = \frac{\gamma\cos\vartheta}{4\mu}R \tag{11}$$

that can be integrated, using $\ell = 0$, at $t = 0$, providing the solution

$$\ell = \left(\frac{\gamma R\cos\vartheta}{2\mu}t\right)^{1/2}. \tag{12}$$

This is Washburn solution, valid only for

$$t >> t_\mu$$

where $t_\mu = \rho R^2/\mu$ is the viscous time scale. The exact and Washburn solutions, Eqs (10) and (12), might be used to verify the accuracy and reliability of any proposed numerical method.

3.2. Entrapped gas action

The entrapped gas action can be taken into account by adding to the right hand side of Eq. (9) the pressure that this gas applies to the penetrant liquid meniscus or by taking into account the viscous drag produced by the gas.

1. Deutsch [13] proposed to use the following term

$$\Omega(\ell, L) = p_a - p_e \,, \tag{13}$$

where p_a is the atmospheric pressure, and entrapped gas pressure

$$p_e = \frac{p_a L}{L - \ell} \tag{14}$$

verifies the initial condition $p_e(\ell = 0) = p_a$, the asymptotic condition

$$\lim_{L \to \infty} p_e = p_a \,, \tag{15}$$

and the limit condition

$$\lim_{\ell \to L} p_e = +\infty \tag{16}$$

corresponding to the common intuition that no action is expected if the capillary is not closed and that the internal pressure will increase if we let ℓ increase for a closed-end capillary. The velocity can be found to be

$$u(r, x) = f(r) \frac{2\gamma \cos \vartheta (L - x) - p_a x R}{L R (L - x)} \tag{17}$$

with

$$f(r) = \frac{R^2}{4\mu} (1 - r^2/R^2) \tag{18}$$

Equations (17) and (18) show that the flow develops slowly enough to retain the parabolic profile of Poiseuille flow, while it adjusts, continuously, its magnitude (and flow rate) in proportion to a constantly diminishing pressure gradient. From equation (17) we note that the flow will cease when

$$\frac{x}{L} = \frac{2\gamma \cos \vartheta}{R p_a + 2\gamma \cos \vartheta}. \tag{19}$$

According to Deutsch [13], for p_a of one atmosphere (≈ 101325 Pa), $R = 100$ μm and an air-water interface, equation (19) shows that the flow will cease at

$$\frac{\ell_{\max}}{L} \approx 1.5\% \,, \tag{20}$$

and there will be about 98.5% of free capillary depth to be filled by a second penetrant liquid.

2. A second way to model the entrapped gas action, due to Zhmud et al. [33], is to take into account the viscous drag produced by the entrapped gas. In this way, it is possible to derive the formula

$$\Omega(\ell, L) = \frac{8\mu_e (L - \ell)}{R^2} \frac{d\ell}{dt} \,, \tag{21}$$

where μ_e is the viscosity of the entrapped gas. However, in this case we get

$$\lim_{L \to \infty} \Omega = \infty \,,$$

and this contradicts the common intuition that no entrapped gas action should be taken into account for an open ended capillary.

4. Numerical method and adaptive strategy

In this section we describe the considered numerical method as well as the adaptive procedure used. The classical fourth order Runge-Kutta's method [6, p. 166] was implemented with an adaptive procedure developed by Jannelli and Fazio [17]. For the reported test cases we used the following monitor function

$$\eta(t_k) = \frac{\left| \dfrac{d\ell}{dt}(t_k + \Delta t_k) - \dfrac{d\ell}{dt}(t_k) \right|}{\Gamma_k} \tag{22}$$

where Δt_k is the current time-step and

$$\Gamma_k = \begin{cases} \left| \dfrac{d\ell}{dt}(t_k) \right| & \text{if} \quad \dfrac{d\ell}{dt}(t_k) \neq 0 \\ \epsilon & \text{otherwise.} \end{cases} \tag{23}$$

where $0 < \epsilon \ll 1$. The above monitor function has been defined because, for small values of R, we have found numerically that initially the first derivative of $\ell(t)$ has a fast transient.

For the adaptive procedure we enforced the following conditions: $\Delta t_{\min} \leqslant \Delta t_k \leqslant \Delta t_{\max}$ with $\Delta t_{\min} = 10^{-15}$, $\Delta t_{\max} = 1$, and $\eta_{\min} \leqslant \eta(t_k) \leqslant \eta_{\max}$ with $\eta_{\min} = 10^{-2}$ (but $\eta_{\min} = 10^{-4}$ in the two-liquids test cases), $\eta_{\max} = 10 \, \eta_{\min}$, and $\epsilon = 10^{-9}$. Moreover, the time step is modified in two cases: when $\eta(t_k) < \eta_{\min}$ we use $\Delta t_{k+1} = 2 \, \Delta t_k$ as the next time step, whereas if $\eta(t_k) > \eta_{\max}$, then we repeat the same step using $\Delta t_k = \Delta t_k/2$. Full details on the adaptive strategy, as well as alternative monitor functions, can be found in [17] by the interested reader.

5. Numerical results

All computation were performed with MATLAB. Let us consider first a single fluid model.

5.1. One fluid model

As a first academic test case we report on the numerical results for the model Eq. (9)

$$\rho(\ell + cR)\frac{d^2\ell}{dt^2} + \rho\left(\frac{d\ell}{dt}\right)^2 = 2\frac{\gamma\cos\vartheta}{R} - 8\frac{\mu\ell}{R^2}\frac{d\ell}{dt} \, ,$$

supplemented with the following initial conditions

$$\ell(0) = 0 \, , \frac{d\ell}{dt}(0) = 0 \tag{24}$$

and parameters

$$R = 0.01 \, , c = \rho = 2\frac{\gamma\cos\vartheta}{R} = 8\frac{\mu}{R^2} = 1. \tag{25}$$

In the top frame of Fig. 2, we show the numerical solution ℓ, compared with the Washburn equation, and its first derivative. Our adaptive strategy used 1468 steps, plus 10 rejections, to complete the integration
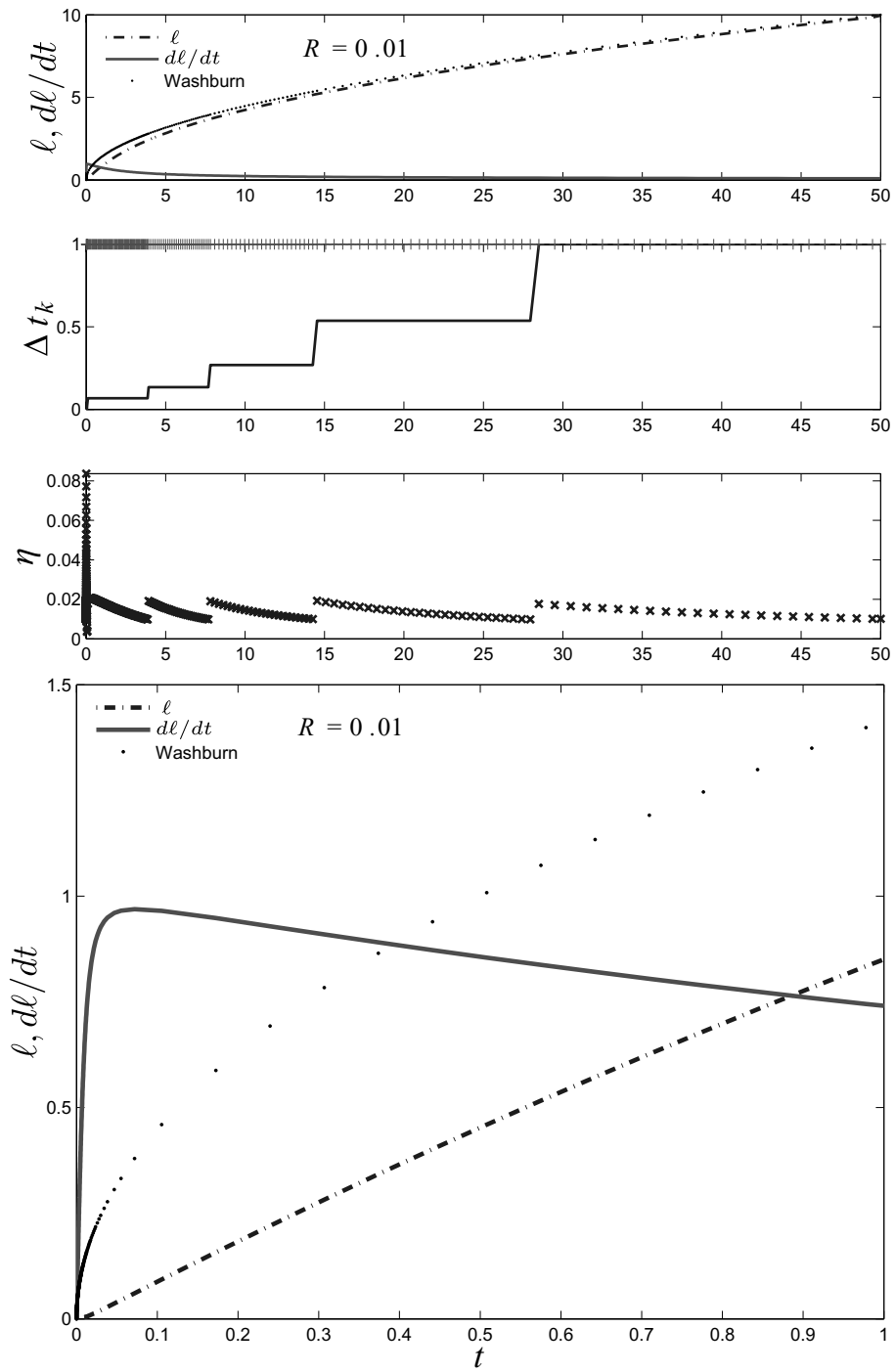
Fig. 2. Adaptive step-size results. From top to bottom: $\ell(t)$ and its first derivative; adaptive step-size selection Δt_k; monitor function η; and zoom of the initial transient of $d\ell/dt$, the $\cdot$ – line is $\ell(t)$, and the $\cdots$ line is the Washburn solution (shown for comparison).

Table 1
Parameters of different liquids according to the recent survey by
Korney and Neimark [19]

Liquid	Viscosity μ (mPa·s)	Density ρ (Kg/m^3)	Surface tension γ (mN/m)	Contact angle ϑ
Silicon oil	500	980	21.1	0°
Ethanol	1.17	780	21.6	0°
Ether	0.3	710	16.6	0°
Mixture	0.77	955	57	10°
Water	1	998	71.8	0°

in $[0, 1]$, but 1613 steps, plus the same 10 rejections, to complete the integration in $[0, 50]$. For this test case, the minimum value of Δt used was about 10^{-12}.

The step-size selection Δt_k and the monitor function $\eta(t_k)$ are reported in the middle frames of this figure. Notice how the adaptive procedure modifies the time step in relation to the value of the monitor function. Initially, at the beginning of the process, the adaptive procedure reduces Δt_k corresponding to fast transitory of first derivative. Then, when the solution becomes smooth, the procedure amplifies the step-size. It can be easily seen, from the magnification at the bottom frame of this figure, that the liquid entering the capillary is accelerated by capillary force ($\ell \approx t^2$ initially); but, soon thereafter the capillary force is compensated by the viscous drag so that a steady-state can be achieved ($\ell \approx t^{1/2}$).

Of course, we have also performed several numerical tests, involving the parameters characterizing different real liquids as well as the entrapped gas pressure term. We used the liquid parameters listed in [19] and reported, for the reader convenience, in Table 1. In all the following test cases we use a coefficient of apparent mass $c = 7/6$. Figure 3 shows the initial transient for several values of the capillary radius for the case of a mixture of penetrant liquid. It can be easily seen that: the smaller the radius R is, the steeper the transient is and the faster the solution ℓ approaches the Washburn solution. Let us notice how the particular case reported in literature (that is the top-left frame of Fig. 3) is, from a numerical viewpoint, the easiest among the four considered cases. Moreover, by comparing the bottom frame of Fig. 2 to the top-left frame of Fig. 3, we can realize that the academic test case presented above, where the only parameter to be varied is R, can be used to trial different numerical methods.

As a third test case, Fig. 4 shows numerical results corresponding to a closed-end capillary and water, see Deutsch [13]. We remark that the obtained result $\ell_{\max}/L \approx 1.4\%$ is thinly different from Deutsch one, because we have taken into account also the effect due to the apparent mass, that is $c \neq 0$, which is related to the outside flow dynamics. Depending on R and L, we have also observed the occurrence of oscillatory solutions, according with the experimental data reported by Zhmud et al. [33], verifying the reported condition: $\ell_{\max}/L \approx 1.4\%$.

In the next section, we describe two test cases for the two-fluids model.

5.2. Two-fluids model

Here, we report on the numerical results for the model Eq. (7), that is

$$\frac{d}{dt}\left[(\rho_1\ell_0 + \rho_2(\ell + cR))\frac{d\ell}{dt}\right] = 2\frac{\gamma_1\cos\vartheta_1 + \gamma_{12}\cos\vartheta_{12}}{R} - 8\frac{\mu_1\ell_0 + \mu_2\ell}{R^2}\frac{d\ell}{dt} \,,$$

with the initial conditions

$$\ell(0) = 0 \,, \frac{d\ell}{dt}(0) = 0 \,,$$
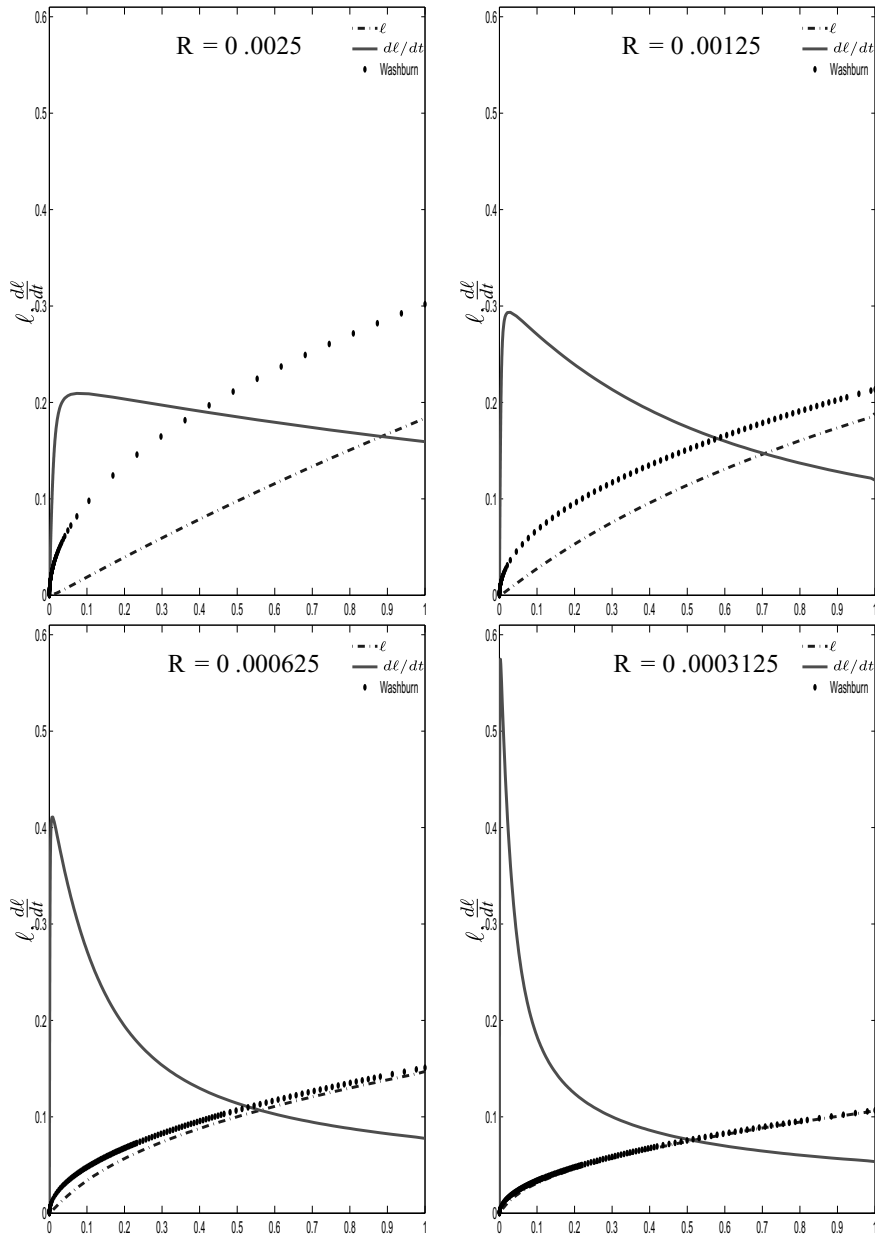
Fig. 3. Results by halving several times the value of $R = 0.0025$ (top-left frame). Parameters listed in Table 1 for a mixture of penetrant liquid.

and parameters listed in Table 1.

Several test cases were considered where water was always in front of the other liquid. Two simulations related to ethanol and water and mixture and water are available in [15]. Here we report instead the cases involving silicone oil and water, and ether and water. With reference to Fig. 5, which shows the case with ether and water, and 6, showing the one with silicone oil and water, we notice that the monotone functions are $\ell(t)$ and $\ell_0(t)$; the fast transient of the first derivative of ℓ is characteristic for this kind of
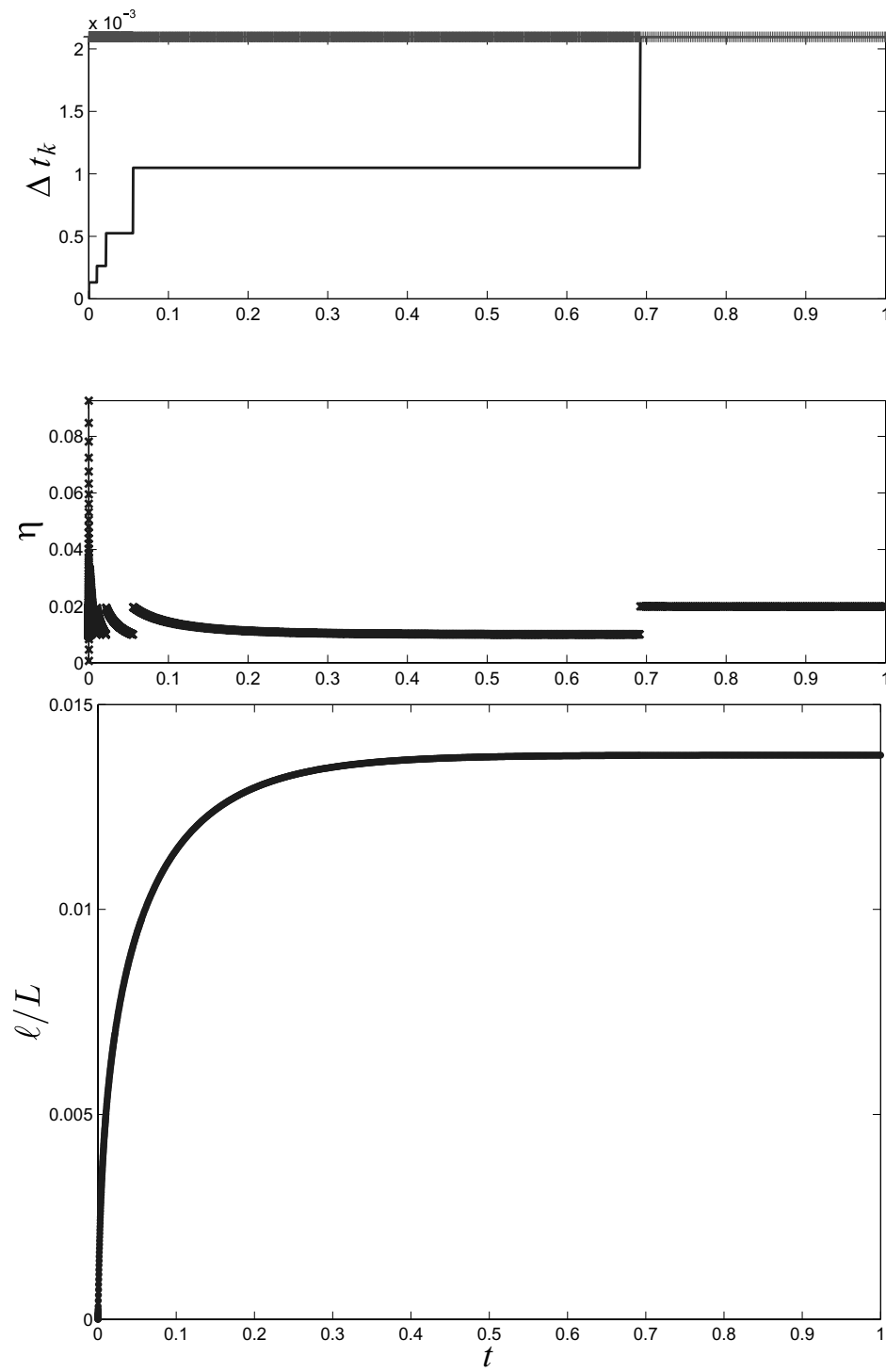
Fig. 4. Water simulation in a close-end capillary: step selection and monitor function on the top two frames, and $\ell(t)/L$ on the bottom frame.
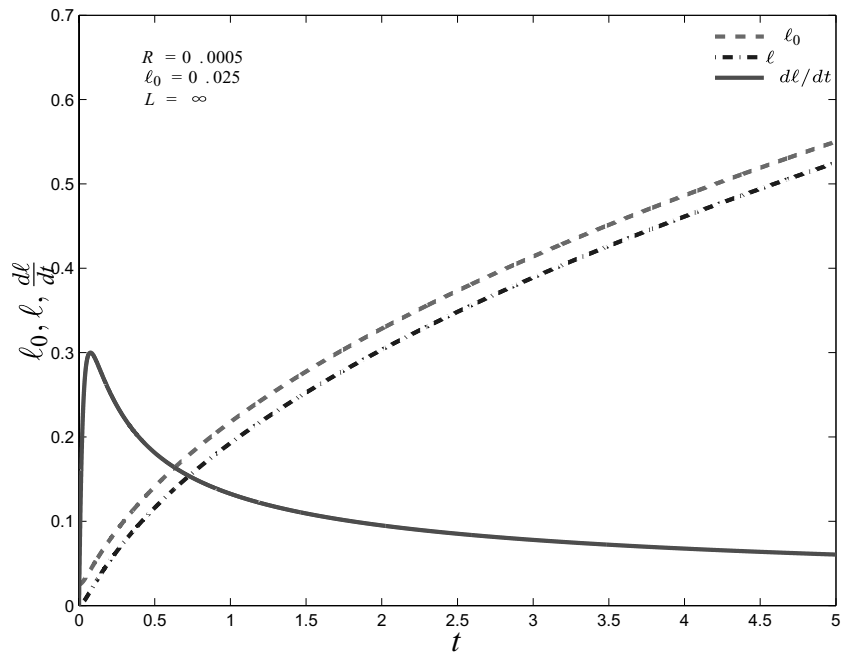
Fig. 5. Open capillary with $\ell_0(\theta) = 0.025$, and $R = 0.0005$: ether and water.
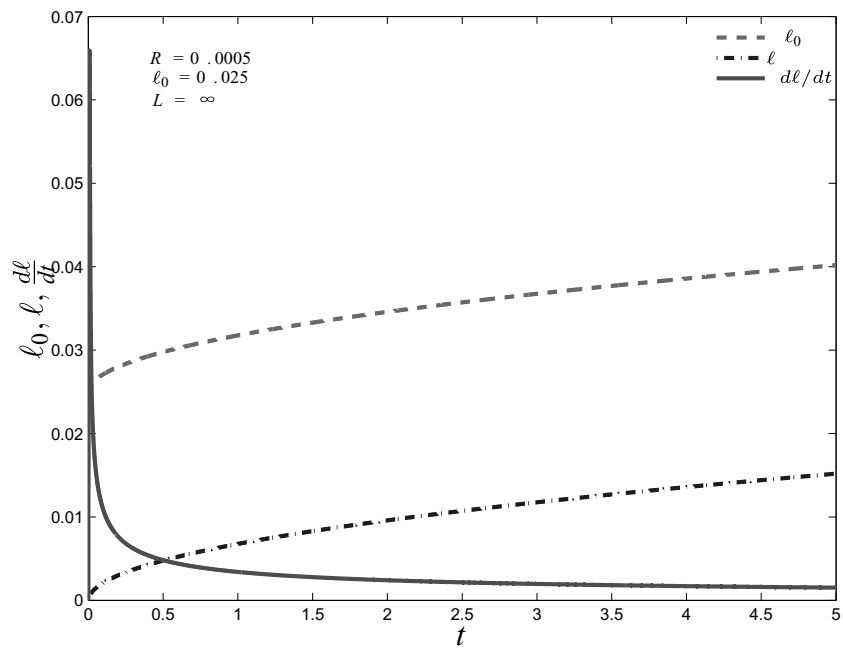
Fig. 6. Open capillary with $\ell_0(\theta) = 0.025$, and $R = 0.0005$: silicone oil and water.

problems. The different behavior of the solutions in the two figures can be explained as follows: the ether, having a surface tension of the same oder of magnitude but a much lower viscosity with respect to the silicone oil, reaches a dipper distance inside the capillary than the one reached by silicone oil.

6. Concluding remarks

In this paper we have proposed a simple derivation, from first principles, of one-dimensional mathematical models of capillary dynamics. In Section 3 we reported the classical result of a single fluid related to the Washburn solution. The effects of the inertial terms, neglected by Washburn equation, show how, at the beginning of the process, the liquid entering in the capillary is accelerated. In fact, for small values of the capillary radius, the first derivative of the meniscus location presents a fast transient. We showed the influence of the capillary radius on the initial transient in the case of a mixture of penetrant liquid. The smaller the radius is, the steeper the transient is.

As shown in Section 5, all the proposed versions of the physical model have a first derivative of the field variable with a fast transitory after the starting time. So that, the most important feature of the numerical method applied to the model is its adaptivity, used here to prevent stability problems and to provide uniform accurate results on the time interval of interest.

Acknowledgment

References

[1] A.W. Adamson, *Physical Chemistry of Surfaces*, Wiley, Singapore, 1997.
[2] J.M. Bell and F.K. Cameron, Movement of liquids through capillary tubes, *J Phys Chem* **10** (1906), 658–674.
[3] G. Birkhoff, *Hydrodynamics: A Study on Logic, Fact and Similitude*, Princeton University Press, 1950, Princeton, 2nd edition, 1960.
[4] T.D. Blake and J. De Coninck, The influence of pore wettability on the dynamics of imbibition and drainage, *Colloids and Surfaces A: Physicochem. Eng. Aspects* **250** (2004), 395–402.
[5] C.H. Bosanquet, On the flow of liquids into capillary tubes, *Philos Mag Ser* **6** (1923), 525–531.
[6] J.C. Butcher, *Numerical Methods for Ordinary Differential Equations*, Whiley, Chichester, 2003.
[7] L. Cartz, *Nondestructive Testing*, ASM International, Materials Park, OH, 1995.
[8] G. Cavaccini, V. Pianese, S. Iacono, A. Jannelli and R. Fazio, Mathematical and numerical modeling of liquids dynamics in a horizontal capillary, in: *Recent Progress in Computational Sciences and Engineering, ICCMSE 2006, Lecture Series on Computer and Computational Sciences*, (Vol. 7), T. Simos and G. Maroulis, eds, Leiden, The Netherlands, Koninklijke Brill NV, 2006, pp. 66–70.
[9] W.K. Chan and C. Yang, Surface-tension-driven liquid liquid displacement in a capillary, *J Micromech Microeng* **15** (2005), 1722–1728.
[10] C. Clanet and D. Quéré, Onset of menisci, *J Fluid Mech* **460** (2002), 131–149.
[11] P.G. de Gennes, Wetting: statics and dynamics, *Rev Mod Phys* **57** (1985), 827–890.
[12] P.G. de Gennes, F. Brochard-Wyart and D. Quéré, *Capillarity and Wetting Phenomena*, Springer, New York, 2004.
[13] S. Deutsch, A preliminary study of the fluid mechanics of liquid penetrant testing, *J Res Natl Bur Stand* **84** (1979), 287–292.
[14] E.B. Dussan, On the spreading of liquids on solid surfaces: static and dynamic contact angles, *Ann Rev Fluid Mech* **11** (1979), 371–400.
[15] R. Fazio, S. Iacono, A. Jannelli, G. Cavaccini and V. Pianese, A two immiscible liquids penetration model for surface-driven capillary flows, *PAMM* (*Proc Appl Math Mech*) **7** (2007), 2150003–2150004.

[16] L.R. Fisher and P.D. Lark, An experimental study of the Washburn equation for liquid flow in very fine capillaries, *J Colloid Interf Sci* **69** (1979), 486–492.

[17] A. Jannelli and R. Fazio, Adaptive stiff solvers at low accuracy and complexity, *J Comput Appl Math* **191** (2006), 246–258.

[18] J.A. Mann, Jr., L. Romero, R.R. Rye and F.G. Yost, Flow of simple liquids down narrow V grooves, *Phys Rev E* **52** (1995), 3967–3972.

[19] K.G. Kornev and A.V. Neimark, Spontaneous penetration of liquids into capillaries and porous membranes revisited, *J Colloid Interf Sci* **235** (2001), 101–113.

[20] L. Leger and J.F. Joanny, Liquid spreading, *Reports Progress Phys* **55** (1992), 431–486.

[21] R. Lucas, Über das zeitgesetz des kapillaren Ausfstiegs von Flüssigkeiten, *Kolloid Z* **23** (1918), 15–22.

[22] G. Martic, F. Gentner, D. Seveno, D. Coulon, J. De Coninck and T.D. Blake, A molecular dynamics simulation of capillary imbibition, *Langmuir* **18** (2002), 7971–7976.

[23] A.V. Pesse, G.R. Warrier and V.K. Dhir, An experimental study of the gas entrapment process in closed-end microchannels, *Int J Heat Mass Transf* **48** (2005), 5150–5165.

[24] K.A. Polzin and E.Y. Choueiri, A similarity parameter for capillary flows, *J Phys D: Appl Phys* **36** (2003), 3156–3167.

[25] E.K. Rideal, On the flow of liquids under capillary pressure, *Philos Mag* **44** (1922), 1152–1159.

[26] L.A. Romero and F.G. Yost, Flow in an open channel capillary, *J Fluid Mech* **322** (1996), 109–129.

[27] R.R. Rye, F.G. Yost and J.A. Mann, Jr., Wetting kinetics in surface capillary grooves, *Langmuir* **12** (1996), 4625–4627.

[28] R.R. Rye, F.G. Yost and E.J. O'Toole, Capillary flow in irregular surface grooves, *Langmuir* **14** (1998), 3937–3943.

[29] J. Szekely, A.W. Neumann and Y.K. Chuang, The rate of capillary penetration and the applicability of the Washburn equation, *J Colloid Interf Sci* **35** (1971), 273–278.

[30] G.A. Tokaty, *A History and Philosophy of Fluid Mechanics*, Dover, New York, 1994.

[31] E.W. Washburn, The dynamics of capillary flow, *Phys Rev* **17** (1921), 273–283.

[32] F.G. Yost, R.R. Rye and J.A. Mann, Jr., Solder wetting kinetics in narrow V-grooves, *Acta Materialia* **45** (1997), 5337–5345.

[33] B.V. Zhmud, F. Tiberg and K. Hallstensson, Dynamics of capillary rise, *J Colloid Interf Sci* **228** (2000), 263–269.